Pakistan Journal of Scientific Research
Multidisciplinary & Peer Reviewed
Volume: 4, Number: 2(Suppl.), Pages: 16-25, Year:2025

Article

Parametric Optimization of GTAW-welded ASTM A192 Boiler Tubes Using Response Surface Methodology

Hassan Moeez [1, *], and Shahid Mehmood [1]

[1] Mechanical Engineering Department, University of Engineering and Technology, Taxila, Pakistan
* Correspondence: Hassan.moeez@students.uettaxila.edu.pk

Submitted: 10-05-2025**, Revised:** 20-07-2025, **Accepted:** 30-05-2025

Abstract

Heavy Mechanical Complex Taxila (HMC) has long struggled with inconsistent weld quality rates on ASTM A192 boiler tubes. To resolve these challenges, this study employs Response Surface Methodology (Central Composite Design) to systematically optimize Gas Tungsten Arc Welding (GTAW) parameters, together with a controlled pre-heating routine to ensure uniform microstructure. A designed experimental matrix explored the effects of welding current, shielding-gas flow rate, and filler-metal selection on tensile strength and hardness. Statistical analysis revealed that a welding current of 153 A, a shielding-gas flow rate of 16.9 L/min, and the use of ER70S-6 filler consistently achieved tensile strengths above the ASTM A192 minimum while producing homogeneous, defect-free welds under shop conditions. Analysis of variance confirmed that this parameter set significantly reduces defect rates and shortens production cycles. This study reveals the range for welding current (140A-160A) and gas flow rate (15-17 L/min) to obtain optimum UTS and Hardness in ASTM A192 GTAW welded joints.

Keywords: Response Surface Methodology, Central Composite Design (CCD), Analysis of Variance

1. Introduction

Gas Tungsten Arc Welding (GTAW), also referred to as Tungsten Inert Gas (TIG) welding, is a non-consumable electrode welding technique renowned for producing high-quality, defect-free joints. In this process, a stable arc is established between a tungsten electrode and the base metal, generating the heat required to melt the workpiece. A shielding gas, typically Argon or Helium, is delivered through a directed nozzle to protect the molten weld pool from atmospheric contamination, thereby ensuring structural integrity. The GTAW process is especially advantageous in fabricating components where surface finish, metallurgical integrity, and dimensional accuracy are of utmost importance, such as in aerospace, petrochemical, shipbuilding, and pressure vessel industries [1][2].

Unlike consumable electrode methods, GTAW allows precise control over heat input and filler addition, making it well-suited for joining thin-walled structures and dissimilar metals, including stainless steel, carbon steel, aluminum, and copper alloys [3]. This versatility, combined with the superior quality of the welds, underscores its increasing adoption in advanced manufacturing systems. A critical feature of GTAW is its adaptability across a wide range of metals, including complex alloys like AISI 304 and Monel 400, where different filler compositions directly impact residual stresses, hardness, and tensile properties of the welds [4][5]. Nonetheless, despite its many advantages, GTAW is not without limitations. Its success heavily relies on careful

 https://doi.org/10.57041/xxxxx

selection and control of process parameters such as welding current, gas flow rate, electrode polarity, and filler material—each of which can significantly influence mechanical responses like ultimate tensile strength (UTS), hardness, and microstructural evolution of the weldment [6][7].

One of the major concerns in industrial welding, especially within high-pressure boiler and piping systems, is the frequent rejection of weld joints due to inconsistent or suboptimal mechanical properties. This issue is particularly relevant in critical applications involving A192 boiler tubes, which demand exceptional strength, ductility, and pressure resistance. At the Heavy Mechanical Complex Taxila's fabrication shop, inconsistencies in the mechanical performance of GTAW joints, often attributed to poor parameter selection, lead to weld rejections and operational inefficiencies. The A192 carbon steel, characterized by its high-pressure resistance and seamless construction, is used extensively in boilers and superheaters due to its robust chemical and mechanical characteristics [8][9]. However, achieving optimal weld integrity in A192 material requires a finely tuned process window that minimizes defects such as porosity, cracking, and hardness fluctuations.

The ultimate tensile strength (UTS) of GTAW joints is significantly influenced by welding parameters such as current, gas flow rate, bevel angle, and filler material composition. Numerous studies have demonstrated that welding current is often the most dominant factor in determining UTS. For instance, Balaji et al. achieved a maximum UTS of 575.57 MPa at a current of 110 A, bevel angle of 60°, and gas flow rate of 0.7 LPM, indicating that moderate heat input produces optimal mechanical strength [10]. Similarly, Sathish et al. emphasized that gas flow rate has a strong influence on UTS, with optimal strength occurring at a current range of 110–115 A and gas flow rate of 12.5 LPM [11]. Taguchi and response surface methods have been widely used to determine optimal parameter sets for specific materials like AISI 304, SS316L, and AA6351 alloys, with UTS values ranging from 230 MPa to over 600 MPa depending on process settings [12][13][14]. The selection of filler material also plays a vital role; for example, the presence of deoxidizing elements like Si and Mn in ER70S-6 enhances strength by refining microstructure [15]. These findings reinforce the importance of parameter optimization in achieving reliable, high-strength welds suitable for industrial applications.

Hardness is a critical property of welded joints, influencing wear resistance, fracture behavior, and overall structural integrity. In GTAW, hardness is notably affected by process variables such as welding current, filler material, and gas flow rate. Studies on dissimilar joints, such as aluminum-magnesium or carbon steel-stainless steel, have revealed that localized hardness values vary significantly across the weld zone, heat-affected zone (HAZ), and base metal due to thermal gradients and solidification rates [16][17]. For instance, Peng Liu et al. observed that hardness in the Mg fusion area reached HM 275–300, while the aluminum side exhibited lower values between HM 160–200 [17]. Similar patterns were observed in A516-Gr70 and 304 SS welds, where optimized parameters like current (130 A), speed (9.4 cm/min), and gas flow (15 LPM) produced desirable hardness distributions [18]. Moreover, studies suggest an inverse relationship between tensile strength and hardness in some alloys—where increased ductility often corresponds to reduced hardness [16]. Filler material also plays a critical role; alloying elements in consumables like ER70S-6 promotes finer microstructures, thereby increasing hardness without inducing brittleness. Overall, precise control of input variables is essential to tailor hardness profiles that match the service conditions of the welded structure, especially in pressure vessels, pipelines, and critical mechanical assemblies.

Microstructural characteristics of welded joints are directly influenced by the energy input and thermal history during GTAW, which are governed by process parameters such as current, travel speed, heat input, and filler material. These factors affect the size, shape, and distribution of grains in the weld zone and HAZ, thereby altering mechanical performance. For example, high heat input tends to produce coarse grains and wider HAZs, which increase ductility but may reduce tensile strength and hardness [19]. In stainless steel welds, microstructural changes like dendritic formation and ferrite-austenite transformations have been observed with varying current and filler materials, particularly in AISI 304 and duplex alloys [20][21]. Comparative studies between

GTAW and other welding methods such as MIG or resistance spot welding have shown that GTAW typically results in larger HAZ due to slower cooling rates, though it offers better control over phase transformations [22]. The choice of filler wire further impacts microstructure; fillers rich in nickel or with specialized compositions (e.g., ENiCu-7 vs. E309L) influence grain refinement and reduce defects like porosity or cracking [23]. Advanced imaging methods like SEM and ultrasonic testing have confirmed these microstructural trends. Therefore, understanding and manipulating the microstructure through parameter control is essential for ensuring weld integrity, especially in high-performance applications.

This research builds upon existing knowledge by focusing on the parametric optimization of GTAW in welding A192 boiler tubes, employing RSM to investigate and model the influence of welding current, shielding gas flow rate, and filler metal selection on mechanical properties. The goal is to improve weld quality and reliability while minimizing rejections in industrial settings. The selected approach integrates statistical modelling, regression analysis, and experimental validation to develop an efficient, repeatable welding strategy that meets industrial performance standards.

2. Materials and Methods

This research employs a structured experimental methodology to investigate the influence of selected Gas Tungsten Arc Welding (GTAW) parameters on the mechanical properties of ASTM A192 boiler tubes. The methodological framework was established through extensive literature review, which helped identify three critical process variables: welding current, shielding gas flow rate, and filler material type. These variables were selected due to their documented impact on weld strength, hardness, and microstructure. To effectively model and optimize these parameters, Response Surface Methodology (RSM) was employed using a Central Composite Design (CCD) approach, enabling efficient experimentation and robust statistical analysis. A total of 26 experimental runs were designed and executed using Design Expert software (v10.0.5), which facilitated the generation of regression models and analysis of variance (ANOVA) to determine the statistical significance of each input factor on the observed responses.

The experimental work was performed using a LINCOLN ELECTRIC V270-T TIG welding inverter, capable of both Stick and TIG modes with an amperage range of 5–270 A. The setup included standard components such as the GTAW power source, tungsten electrode torch, argon gas cylinder, and precision flow meter to regulate gas flow rate. The experimental variables were welding current (ranging from 90 to 180 A), shielding gas flow rate (11 to 18 liters per minute), and two filler metals—ER70S-2 and ER70S-6—both with a constant filler rod diameter of 1.6 mm. Constant parameters throughout all trials included DC negative polarity (straight polarity), Argon shielding gas, and a V-groove joint configuration. These controls ensured consistency and minimized confounding effects during data collection.

The material selected for this research was ASTM A192 carbon steel boiler tubes, cut into sections of 60 mm length with a 50 mm outer diameter. A192 was chosen for its wide usage in high-pressure and thermal environments such as boilers and superheaters, and its mechanical characteristics include a minimum tensile strength of 325 MPa, yield strength of 180 MPa, and elongation of 35%. Prior to welding, V-grooves were machined at the joint interfaces to facilitate deep weld penetration and even filler distribution. The welding was performed at room temperature on both sides of each joint to improve strength and simulate actual industrial practice. Precise gas flow was maintained using the flow meter, and welding current was adjusted on the inverter control panel. The fine-point tungsten electrode was ground before each weld to maintain a consistent arc profile and improve arc stability.

To analyze the impact of welding parameters, samples from each experimental run were prepared and subjected to standardized mechanical testing. Tensile test specimens were extracted from the welded joints according to ASTM E8M-08 standards.

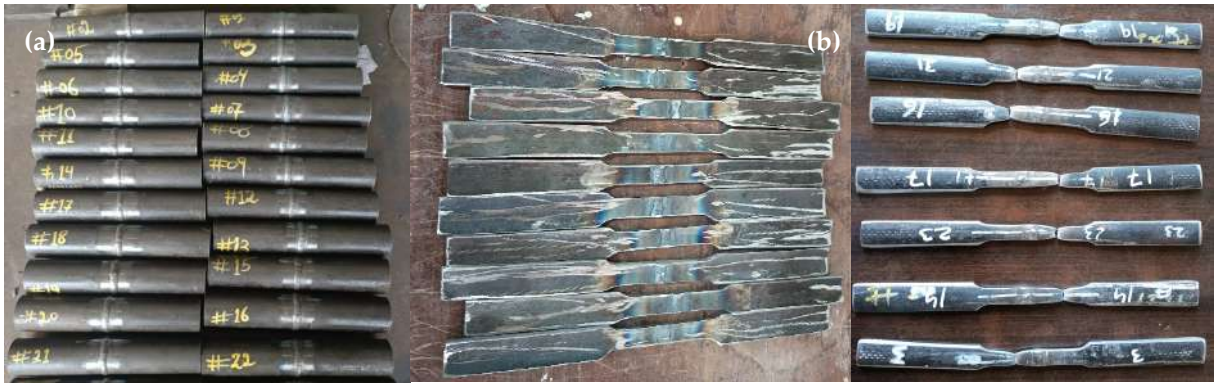

Figure 1: (a) Welded specimens, (b) Cut specimens for Tensile testing, and (c) fractured specimens after tensile testing.

These samples were machined using conventional milling techniques to ensure dimensional conformity and repeatability. The tensile tests were conducted using a universal testing machine to determine the ultimate tensile strength (UTS) of each joint, which served as a primary response variable. Figure 1 shows the specimens after welding, cut specimens before tensile testing, and fractured specimens after tensile testing. Hardness testing was also performed on all specimens using the Rockwell 'B' scale, suitable for evaluating low-carbon steels like A192. The hardness tests provided insight into the influence of filler material and heat input on surface and near-surface hardness distribution.

The statistical design incorporated CCD with axial, factorial, and center points to capture both linear and quadratic effects of the input variables. The total number of runs was determined using the standard CCD formula $2^k + 2(k) + m$. where k is number of factors and m is number of center points which is usually 4-6, resulting in 26 runs. The welding current, gas flow rate, and filler metal were varied systematically according to the CCD matrix, with some values exceeding the central operating range to assess the behavior of the responses under extreme conditions. ANOVA was conducted on the experimental data to evaluate the individual and interaction effects of process variables. Significance levels (p-values) were computed for each parameter, and regression models were developed to predict the tensile strength and hardness outcomes as a function of the input settings.

The robustness of the developed models was evaluated using diagnostic tools such as residual plots, R-squared values, and adequate precision ratios. The predictive models allowed for the generation of 3D response surface and contour plots, visualizing the interaction effects among the variables. These plots helped identify optimal regions in the design space that yield maximum strength and desirable hardness without compromising weld integrity. A validation step was performed by conducting confirmation experiments at the predicted optimal settings, comparing actual results with model predictions to assess the model's reliability.

3. Results and Discussion

In this study, statistical modeling played a vital role in understanding and predicting the behavior of mechanical properties during the Gas Tungsten Arc Welding (GTAW) of ASTM A192 boiler tubes. To achieve accurate and data-driven conclusions, Response Surface Methodology (RSM) with Central Composite Design (CCD) was utilized for experimental planning. The main objective of developing these models was to capture the relationship between three key process variables—welding current, shielding gas flow rate, and filler material—and their combined effect on two critical responses: ultimate tensile strength (UTS) and hardness. Multiple regression models were evaluated for both UTS and hardness. These included linear, 2-Factor Interaction (2FI), quadratic, and cubic models. Based on Analysis of Variance (ANOVA) results, the quadratic model was selected as the most appropriate for both responses. The selection was supported by high F-values and p-values significantly less than 0.005, indicating strong statistical significance. Moreover, the

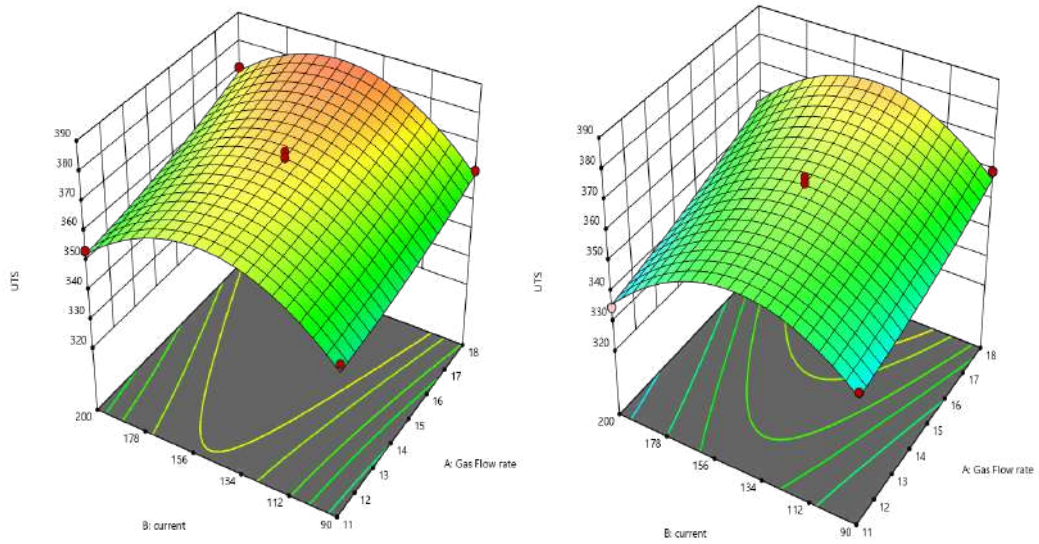

Figure 2: Surface plot of current vs gas flow rate for UTS of ER70s-6 (left) and for ER70s-2 (right).

lack-of-fit test results confirmed that the quadratic models provided a good fit to the experimental data, without overfitting.

For UTS, the selected model achieved an exceptionally high R^2 value of 0.9907, signifying that over 99% of the variability in tensile strength could be explained by the input variables. Similarly, the model for hardness showed a strong R^2 of 0.9223, also indicating a high level of prediction accuracy. In both cases, adjusted R^2 values were close to the actual R^2, confirming the model's consistency, while adequate precision values—used to measure signal-to-noise ratio—exceeded the threshold value of 4, confirming model adequacy for optimization tasks.

These models were not only useful for understanding individual parameter effects but also for revealing interactions between them. For instance, the interaction between current and gas flow was found to significantly influence both UTS and hardness. The models enabled visualization of these effects through surface and contour plots, helping identify the regions of maximum performance. Importantly, the models were validated through confirmation experiments. Predicted values of UTS and hardness were compared against actual measurements at selected process settings. In all cases, the deviation between predicted and experimental values was within 2%, confirming the

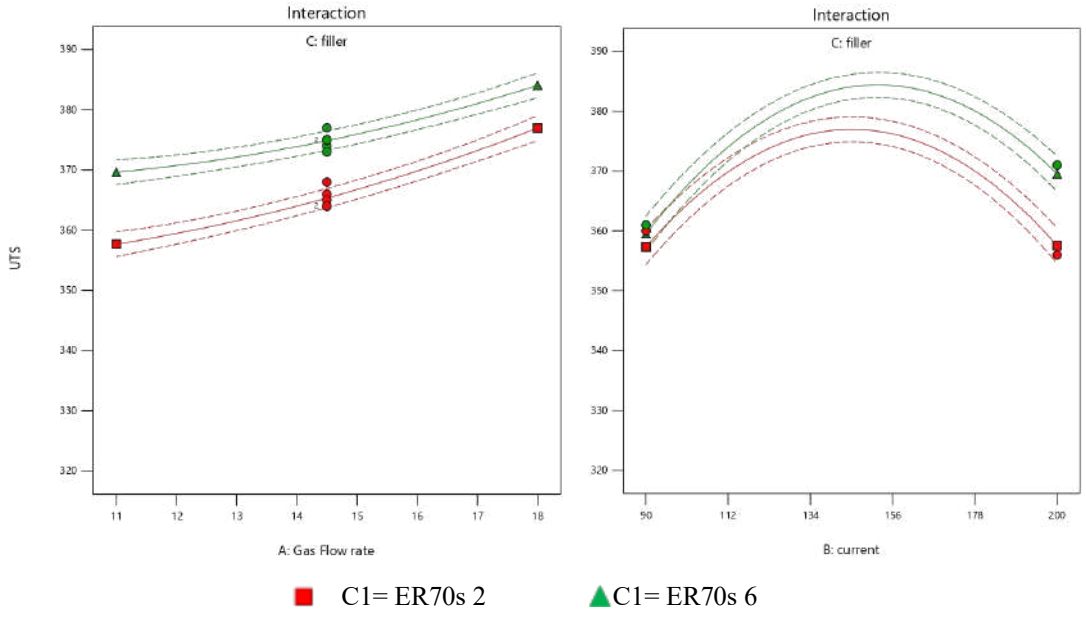

Figure 3: Plot of gas flow rate vs UTS (Left) and Plot of Current vs UTS (Right) with respect to filler material.

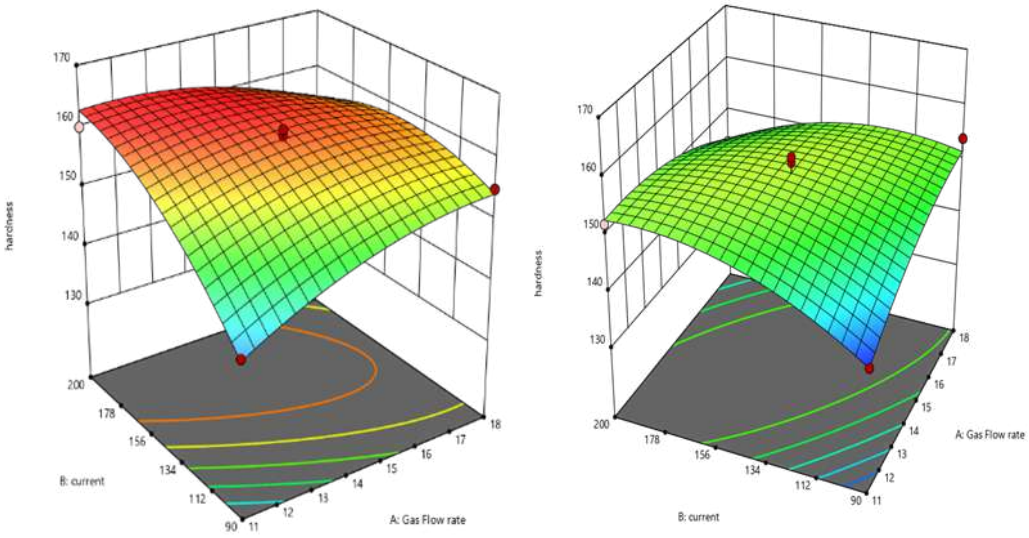

Figure 4: Surface plot of current vs gas flow rate for hardness of ER70s-6 (left) and for ER70s-2 (right).

models' practical reliability. Therefore, the regression models developed through RSM served as powerful tools—not only for analysis but also for optimizing welding conditions to achieve consistent, high-quality welds in a controlled and replicable manner.

The variation in Ultimate Tensile Strength (UTS) in response to changes in welding current and gas flow rate was extensively analyzed using response surface plots and interaction graphs. These relationships were visualized for both ER70S-6 and ER70S-2 filler materials, providing valuable insights into how each parameter influences weld strength. As shown in Figure 2, the surface plots illustrate how UTS responds to the combined effects of current and gas flow rate. For ER70S-6, the UTS values reach their highest levels—typically between 470 and 520 MPa—when both parameters are maintained within a specific mid-range window. Specifically, welding currents between 140 and 160 A and gas flow rates between 15 and 17 L/min yielded the best results. This region of the surface plot is characterized by a smooth plateau, indicating that small fluctuations within this window do not drastically affect performance, provided the balance is maintained. The elevated strength in this range is attributed to ER70S-6's high silicon and manganese content, which promote better arc stability, deeper penetration, and refined microstructures.

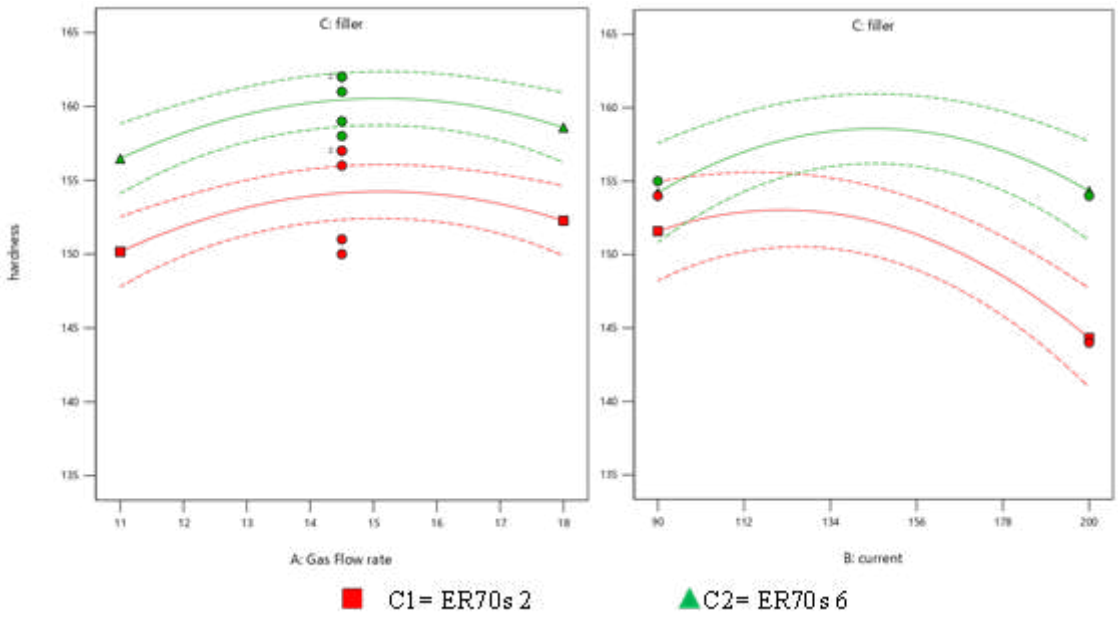

Figure 5: Gas flow Rate Vs Hardness (Left) and Current Vs hardness (Right).

In contrast, the UTS surface plot for ER70S-2 shows a broader, more gradual peak, with tensile strength typically ranging from 400 to 480 MPa. [24] While its maximum strength is lower than that of ER70S-6, the transition across different parameter combinations is smoother, indicating that ER70S-2 offers more consistent performance even when parameters vary. This filler's aluminum-based deoxidation contributes to a stable weld pool and reduces the sensitivity of UTS to process fluctuations.

Figure 3 provides additional clarity through interaction plots, comparing UTS across varying currents and gas flow rates with respect to the filler material. The left graph shows how UTS increases for both fillers as gas flow improves, peaking around 16–17 L/min. ER70S-6 shows a sharp rise and fall, while ER70S-2 remains relatively flat, reinforcing its higher tolerance to shielding conditions. On the right-hand graph, the influence of welding current is more prominent. ER70S-6 again shows a steeper curve, peaking in the 150–160 A range and then declining beyond this due to overheating and potential microstructural degradation. ER70S-2 follows a steadier, less aggressive slope, again reflecting its greater resilience to variations in heat input. Overall, ER70S-6 provides higher UTS but within a narrower process window, while ER70S-2 offers stable performance across broader parameter ranges, making it suitable for less controlled environments. [25].

Table 1. Confirmation results for UTS and hardness (HRB).

Run	Welding Current (Amp)	Gas Flow Rate (lit/min)	Filler material	UTS (MPa)			Hardness (HRB)		
				Experimental	Predicted	Error %	Experimental	Predicted	Error %
1	140	15	ER70s-2	366	370	1.08	154	152	1.39
2	150	18	ER70s-6	384	378	1.32	158	161	1.53

The response of weld hardness to variations in welding current and gas flow rate was analyzed for both ER70S-6 and ER70S-2 filler materials. The surface plots and interaction graphs offer critical insight into how each process variable influences the hardness of GTAW welds on ASTM A192 boiler tubes. Figure 4 presents the 3D surface plots for hardness with respect to changes in current and gas flow rate. For ER70S-6, peak hardness values—ranging between 178 and 200 HRB—are observed when the welding current is maintained between 140 and 160 A, and the gas flow rate is kept between 15 and 17 L/min. This narrow range forms a high-performance zone where the combined thermal input and effective shielding promote fine microstructure formation and solid-solution strengthening. However, deviations outside this optimal range lead to a noticeable drop in hardness. At current levels below 130 A, the arc energy becomes insufficient for proper fusion, resulting in weaker and softer welds [26][27]. Conversely, increasing the current beyond 170 A causes thermal overloading, which can lead to grain coarsening and reduced hardness. Similarly, gas flow rates below 14 L/min compromise shielding, allowing atmospheric contamination, while flow rates above 17 L/min introduce turbulence, both of which degrade weld quality [28][29].

For ER70S-2, the surface plot shows a more gradual increase in hardness with changing parameters. Maximum values typically range between 160 and 175 HRB. The optimal hardness region for this filler material spans a broader range of conditions, reflecting its greater tolerance to parameter fluctuations. This resilience is mainly due to the presence of aluminum, which provides robust deoxidation and improves the filler's adaptability to varied welding conditions. These observations are further supported by the interaction plots shown in Figure 5. The left graph illustrates the effect of gas flow rate on hardness. ER70S-6 exhibits a steep increase in hardness up to the optimal range, followed by a decline at higher flow rates. In contrast, ER70S-2 shows a flatter response curve, maintaining relatively consistent hardness even as shielding gas conditions change [30]. The graph on the right displays the relationship between welding current and hardness. Again, ER70S-6 reaches higher hardness values within a narrow current band but shows sharp drops

outside it. ER70S-2, [25] on the other hand, gradually increases in hardness with current, with less pronounced fluctuations.

To validate the reliability and accuracy of the developed regression models for Ultimate Tensile Strength (UTS) and hardness, confirmation experiments were performed under optimized process settings. The goal was to compare the predicted values generated by the models with the actual experimental measurements and evaluate the percentage deviation between the two. Two validation runs were conducted, each using one of the filler materials—ER70S-2 and ER70S-6. For UTS, the first trial was performed at a welding current of 140 A and gas flow rate of 15 L/min using ER70S-2. The second trial used 150 A current and 18 L/min gas flow with ER70S-6. As shown in Table 1, the UTS values predicted by the model were very close to the actual results, with only 1.08% error for ER70S-2 and 1.32% for ER70S-6. This low margin of error demonstrates the model's high predictive capability and confirms that the quadratic regression approach reliably estimates tensile strength under practical conditions.

A similar validation was carried out for hardness. The same optimized input settings were used for the confirmation tests. According to Table 1, the experimentally observed hardness values were also very close to the model predictions. The error percentage was just 1.39% for ER70S-2 and 1.53% for ER70S-6, again indicating a strong agreement between predicted and actual results. These confirmation results clearly demonstrate that the developed models are both statistically sound and practically applicable. Their ability to closely match experimental outcomes affirms their usefulness in industrial welding environments, where accurate parameter prediction is essential for achieving consistent weld quality. This also validates the response surface methodology as a robust tool for process optimization in GTAW of boiler tubes.

5. Conclusions

This research focused on optimizing Gas Tungsten Arc Welding (GTAW) parameters for ASTM A192 boiler tubes to enhance weld strength and consistency. Using Response Surface Methodology with Central Composite Design, the study systematically analyzed how welding current, gas flow rate, and filler material affect the mechanical properties of the welds. The developed regression models demonstrated strong predictive accuracy for both tensile strength and hardness, confirmed through ANOVA and validation experiments. Among the two filler materials tested, ER70S-6 outperformed ER70S-2 by delivering significantly higher tensile strength and hardness. This improvement is largely due to its higher silicon and manganese content, which enhances solid solution strengthening and microstructure refinement. However, ER70S-2 offered more stable results across a wider range of conditions and showed better tolerance to parameter variations, rendering it preferable for where ductility and flexibility are priorities.

The effects of gas flow and current varied by filler. ER70S-6 required tightly controlled parameters to achieve peak performance, while ER70S-2 was more forgiving, maintaining consistent results across broader ranges. Optimal conditions identified for ER70S-6 involved moderately high current and gas flow rates, ensuring both strength and hardness under shop-floor conditions. Results indicate that welding currents between 140-160 A and gas flow rates between 15-17 L/min yielded the best results for both UTS and hardness. This research provides a validated, statistically robust guideline for industrial GTAW welding of boiler tubes. Future studies can expand on other mechanical properties, explore dissimilar metal welds, and apply advanced optimization tools for broader applications.

References

[1] M. K. Hamjah, "Optimization of new semi-automatic TIG welding process for surface quality through taguchi method.," Universiti Tun Hussein Malaysia., 2014.

[2] I. A. Shaikh and M. V. Rao, "A Review on Optimizing Process Parameters for TIG Welding using Taguchi Method & Grey Relational Analysis," 2013. [Online]. Available: https://www.researchgate.net/publication/367150916

[3] E. R. Bohnart, TIG Handbook for GTAW, Gas Tungsten Arc Welding: Miller Electric Mfg. Company. 2005.

[4] A. Kumar and S. Sundarrajan, "Effect of filler wires on mechanical properties of TIG welded stainless steel joints," J Mater Process Technol, vol. 209, no. 3, pp. 1145–1153, 2009.

[5] Balasubramanian, V. Ravisankar, and V. Reddy, "Effect of filler materials on the performance of gas tungsten arc welded AISI 304," Mater Des, vol. 32, no. 3, pp. 1536–1542, 2011.

[6] J. Joshi, M. Thakkar, and S. Vora, "Parametric Optimization of Metal Inert Gas Welding and Tungsten Inert Gas Welding By Using Analysis of Variance and Grey Relational Analysis," 2014. [Online]. Available: www.ijsr.net

[7] K. Kishore, P. V Gopal Krishna, K. Veladri, and S. Qasim Ali, "ANALYSIS OF DEFECTS IN GAS SHIELDED ARC WELDING OF AISI1040 STEEL USING TAGUCHI METHOD," vol. 5, no. 1, 2010, [Online]. Available: www.arpnjournals.com

[8] "Specification for Seamless Carbon Steel Boiler Tubes for High-Pressure Service," May 2024, doi: 10.1520/A0192_A0192M-24.

[9] "Usage Areas of ASTM A192 Seamless Steel Pipes -." Accessed: Apr. 27, 2025. [Online]. Available: https://milfit.com.tr/en/usage-areas-of-astm-a192/

[10] C. Balaji, S. V. A. Kumar, S. A. Kumar, and R. Sathish, "EVALUATION OF MECHANICAL PROPERTIES OF SS 316 L WELDMENTS USING TUNGSTEN INERT GAS WELDING," 2012.

[11] R. Sathish, B. Naveen, P. Nijanthan, K. Arun Vasantha Geethan, and V. Seshagiri Rao, "Weldability and Process Parameter Optimization of Dissimilar Pipe Joints Using GTAW," International Journal of Engineering Research and Applications (IJERA), vol. 2, pp. 2525–2530, 2012, Accessed: Mar. 23, 2025. [Online]. Available: www.ijera.com

[12] A. K. Hussain, A. Lateef, and M. Javed, "Influence of Welding Speed on Tensile Strength of Welded Joint in TIG Welding Process," 2010.

[13] D. Singh, V. Chaturvedi, and J. Vimal, "Application of Signal to Noise Ratio Methodology for Optimization of Tig Process Parameters," Certified International Journal of Engineering and Innovative Technology (IJEIT), vol. 9001, no. 1, pp. 2277–3754, 2008.

[14] J. Joseph and S. Muthukumaran, "Optimization of activated TIG welding parameters for improving weld joint strength of AISI 4135 PM steel by genetic algorithm and simulated annealing," International Journal of Advanced Manufacturing Technology, vol. 93, no. 1–4, pp. 23–34, Oct. 2017, doi: 10.1007/S00170-015-7599-8/METRICS.

[15] M. W. Fu, J. Lu, and W. L. Chan, "Die fatigue life improvement through the rational design of metal-forming system," J Mater Process Technol, vol. 209, no. 2, pp. 1074–1084, Jan. 2009, doi: 10.1016/J.JMATPROTEC.2008.03.016.

[16] J. Wang, M. X. Lu, L. Zhang, W. Chang, L. N. Xu, and L. H. Hu, "Effect of welding process on the microstructure and properties of dissimilar weld joints between low alloy steel and duplex stainless steel," International Journal of Minerals, Metallurgy and Materials, vol. 19, no. 6, pp. 518–524, Jun. 2012, doi: 10.1007/S12613-012-0589-Z/METRICS.

[17] P. Liu, Y. Li, H. Geng, and J. Wang, "Microstructure characteristics in TIG welded joint of Mg/Al dissimilar materials," Mater Lett, vol. 61, no. 6, pp. 1288–1291, Mar. 2007, doi: 10.1016/J.MATLET.2006.07.010.

[18] N. Kiaee and M. Aghaie-Khafri, "Optimization of gas tungsten arc welding process by response surface methodology," Materials & Design (1980-2015), vol. 54, pp. 25–31, Feb. 2014, doi: 10.1016/J.MATDES.2013.08.032.

[19] S. Kumar, A. S.-M. & Design, and undefined 2011, "Effect of heat input on the microstructure and mechanical properties of gas tungsten arc welded AISI 304 stainless steel joints," ElsevierS Kumar, AS ShahiMaterials & Design, 2011•Elsevier, Accessed: May 03, 2025. [Online]. Available: https://www.sciencedirect.com/science/article/pii/S0261306911000951

[20] V. Anand Rao and R. Deivanathan, "Experimental Investigation for Welding Aspects of Stainless Steel 310 for the Process of TIG Welding," Procedia Eng, vol. 97, pp. 902–908, Jan. 2014, doi: 10.1016/J.PROENG.2014.12.365.

[21] S. Takhti, M. Reihanian, and A. Ashrafi, "Microstructure characterization and mechanical properties of gas tungsten arc welded cast A356 alloy," Transactions of Nonferrous Metals Society of China, vol. 25, no. 7, pp. 2137–2146, Jul. 2015, doi: 10.1016/S1003-6326(15)63825-0.

[22] H. Ghazanfari, M. Naderi, M. Iranmanesh, M. Seydi, and A. Poshteban, "A comparative study of the microstructure and mechanical properties of HTLA steel welds obtained by the tungsten arc welding and resistance spot welding," Materials Science and Engineering A, vol. 534, pp. 90–100, Feb. 2012, doi: 10.1016/j.msea.2011.11.046.

[23] K. Devendranath Ramkumar, N. Arivazhagan, and S. Narayanan, "Effect of filler materials on the performance of gas tungsten arc welded AISI 304 and Monel 400," Mater Des, vol. 40, pp. 70–79, Sep. 2012, doi: 10.1016/J.MATDES.2012.03.024.

[24] A. de A. Vicente, P. A. D'silva, R. Babu, I. L. dos Santos, R. R. de Aguiar, and T. F. de A. Santos, "The correct choice among welding wires ER70S-2, ER70S-3 and ER70S-6, according to the oxidation level of base metal," International Journal of Advanced Engineering Research and Science, vol. 7, no. 8, pp. 131–139, 2020, doi: 10.22161/ijaers.78.15.

[25] M. Tazeem Khan and rd Year, "DESIGN & MANUFACTURING OF FSAE CHASSIS," 2021. [Online]. Available: www.irjmets.com

[26] M. Anto, K. O. Gyimah, B. Addai, A. K. Isaac, M. Owusu, and A. Jnr. Amoako Atta, "The Effect of Welding Current on the Hardness and Tensile Properties of Mild Steel A36LCS TIG Welded Joints: A Comparative Study of Lap and Butt-Welded Joints," European Modern Studies Journal, vol. 7, no. 4, pp. 444–454, Oct. 2023, doi: 10.59573/emsj.7(4).2023.40.

[27] O. Adigun, A. Adebayo, and O. Abiola, "The Effect of Welding Parameter on the Tensile and Impact Properties of Weldments," American Journal of Mechanical and Materials Engineering, vol. 9, no. 1, pp. 37–42, Mar. 2025, doi: 10.11648/j.ajmme.20250901.14.

[28] D. A. Yeshanew, D. A. Yeshanew, and L. M. Mana, "Investigating the effect of TIG welding process variables on the mechanical properties of stainless steel-304 pipe welded joints." Apr. 26, 2024. doi: https://doi.org/10.21203/rs.3.rs-4164082/v1.

[29] M. Nuzan Rizki, R. Putra, and I. Mawardi, "Influence of shielding gas flow on the TIG welding process using stainless steel 304 material," 2024.

[30] M. Pan, Y. Li, S. Sun, W. Liao, Y. Xing, and W. Tang, "A Study on Welding Characteristics, Mechanical Properties, and Penetration Depth of T-Joint Thin-Walled Parts for Different TIG Welding Currents: FE Simulation and Experimental Analysis," Metals, vol. 12, no. 7, Jul. 2022, doi: 10.3390/met12071157.